Two-dimensional Steady Heat Convection

Pratik M Panchal (AM22S033)

October 19, 2022

Assignment - 2

Foundations of CFD (AM5630)

V. D. Narasimhamurthy

Department of Applied Mechanics, IIT Madras

1 Methodology

1.1 Physical description of the problem

The study aims to solve the two-dimensional steady heat convection over the simple rectangular domain with different boundary condition, as shown in Fig. 1(a),(b) and (c). The length (L) and height (H) of computational domain are 2 and 2, respectively.

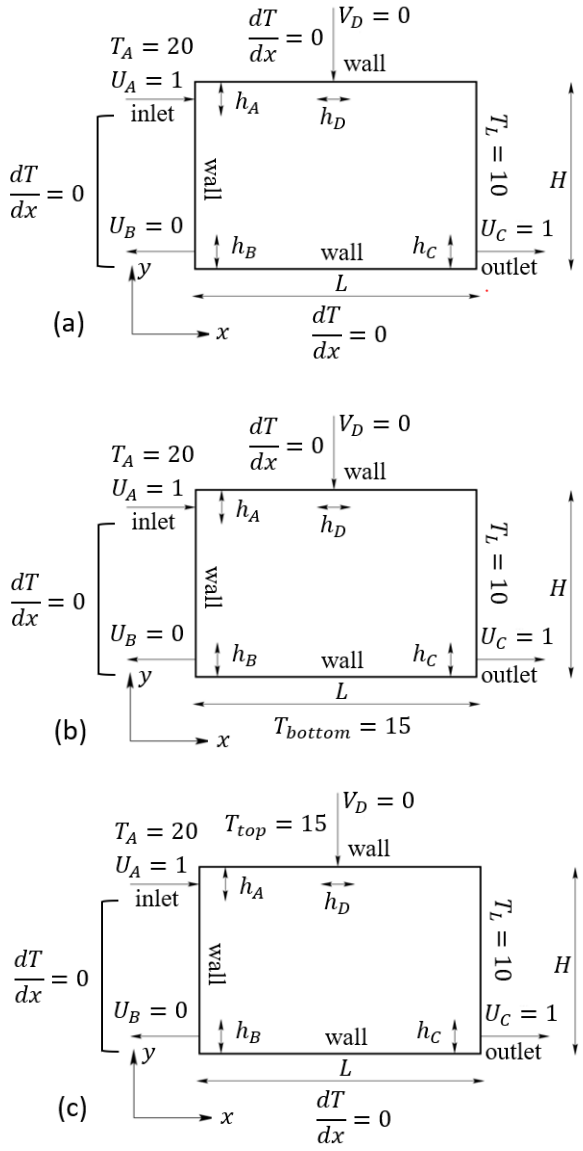

Figure 1: Computational domain for two-dimensional steady heat convection for first problem (a), second problem (b) and third problem (c).

1.2 Governing Equation for heat conduction

The governing equation for the two-dimensional, steady heat convection are as follows:

$$\frac{\partial}{\partial x}(\rho UT) + \frac{\partial}{\partial y}(\rho VT) = \frac{\partial}{\partial x}\left(\Gamma \frac{\partial T}{\partial x}\right) + \frac{\partial}{\partial y}\left(\Gamma \frac{\partial T}{\partial y}\right) + S \tag{1}$$

Here, x and y are coordinates in x and y direction, respectively. T is temperature and heat generation per unit area (S) equals to 0. Γ is thermal diffusion coefficient, defined as ratio of k/C_p. For the first problem, velocity inlet ($U_A = 1$) boundary condition along with temperature dirichlet boundary condition ($T_A = 20°C$) is imposed on the inlet. The insulation boundary condition is applied on left ($^{\mathrm{dT}}/_{\mathrm{dx}} = 0$), top and bottom wall. The velocity outlet ($U_C = 1$) boundary condition is applied on outlet. The dirichlet condition ($T_L = 10°C$) applied on the whole right side of the domain. In the second problem, only the bottom wall neuman boundary condition ($^{\mathrm{dT}}/_{\mathrm{dx}} = 0$) is changed to dirichlet ($T_{bottom} = 15$) with keeping other boundary condition same. While, in the third problem, only the top wall neuman boundary condition ($^{\mathrm{dT}}/_{\mathrm{dx}} = 0$) is changed to dirichlet ($T_{top} = 15$) with keeping other boundary condition same. The mathematical description of boundary conditions for both the problems are given in Fig. 1(a),(b) and (c).

1.3 Numerical details

The governing equations are solved using the Finite Volume Method (FVM) on a cartensian computational grid as shown in Fig. 2. The computational domain is discretized using the non-uniform grid. The simulation is done using C++ code. The central differencing (CD) scheme (second-order) is used to discretize diffusion term and hybrid scheme is used for convection term. The source term is zero in the problem. A simple Gauss- Seidel iterative procedure is used to solve linear system of equation with tolerance of 10^{-6} and the effectiveness of the algorithm is compared with Tridiagonal matrix algorithm (Thomas's algorithm - TDMA) (horizontal and vertical sweep). The results are also compared with different convergence criterion $10^{-3}, 10^{-4}$ and 10^{-6} in Sec. 2.2.

2 Results and Discussion

The present study peformed detail analysis for the first problem in subsequent sections. In the end, the results of first problem is compared with change in one of neuman boundary condition to dirichlet i.e, second and third problem in Subsec. 2.4 and 2.5.

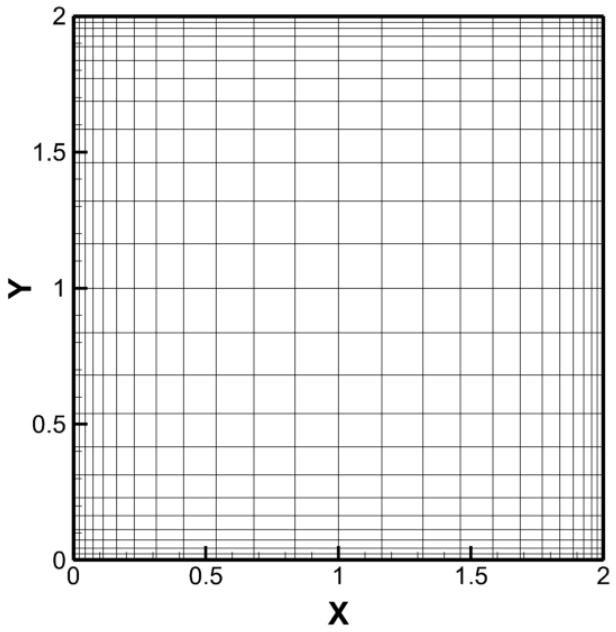

Figure 2: Computational uniform-grid ($40\,X\,20, \Delta x = \Delta y$)

2.1 Effectiveness of algorithm

To verify effectiveness of algorithm, the numerical simulation of two-dimensional steady heat convection is perfomed using both Gauss- Seidel and TDMA alogirthm with considering convergence criterion of 10^{-6}. The residue computed from each iteration is plotted for Gauss- Seidel, horizontal TDMA and vertical TDMA alogirthm as illustracted in Fig. 3. In Fig. 3, it is found that the number of iteration required to converge (convergence criterion -10^{-6}) the solution is less in horizontal TDMA algorithm compared to Gauss- Seidel and vertical TDMA. Thus, we have used horizontal TDMA algorithm to analyse the temperature distribution throughout the domain.

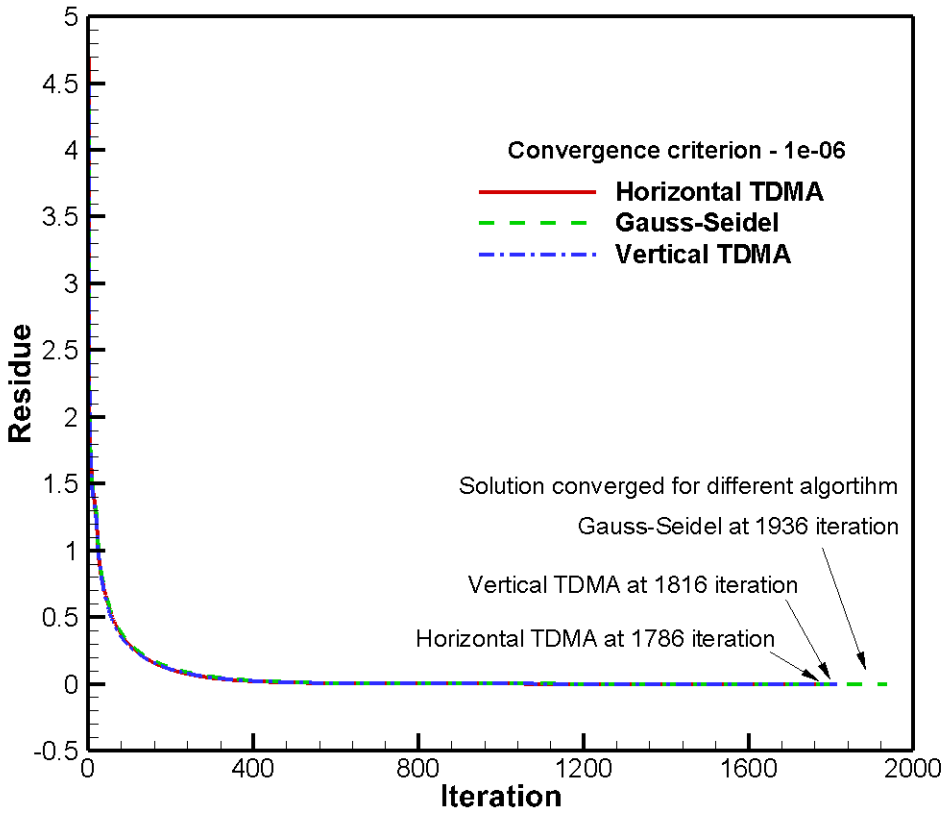

Figure 3: plot of residue against number of interation for different iterative algorithm - Gauss- Seidel, horizontal TDMA and vertical TDMA.

2.2 Effect of different convergence criterion (answer of second question)

In previous Subsec. 2.1, effectiveness of algorithm is compared for numerical simulation using convergence criterion of 10^{-6}. Furthermore, to analyse the effect of convergence criterion on results, we took different tolerance value of 10^{-3} and 10^{-4}. In Figure 4, we compared the temperature variation over a section at $y = H/2$ using horizontal TDMA algorithm, along x-direction for four different tolerance value of of $10^{-3}, 10^{-4}$ and 10^{-6}. It is observed from the figure that the temperature distribution along x-direction for all tolerance values are almost same. However, around $x = 0$ to $x = 0.04$ and $x = 1.8788$ to $x = 1.8794$ (in zoom section of Fig. $4(a)$), temperature is under-predicted for tolerance value of $10^{-3}, 10^{-4}$ compared to 10^{-6}. Therefore, we have taken convergence criterion equal to 10^{-6} for simulation.

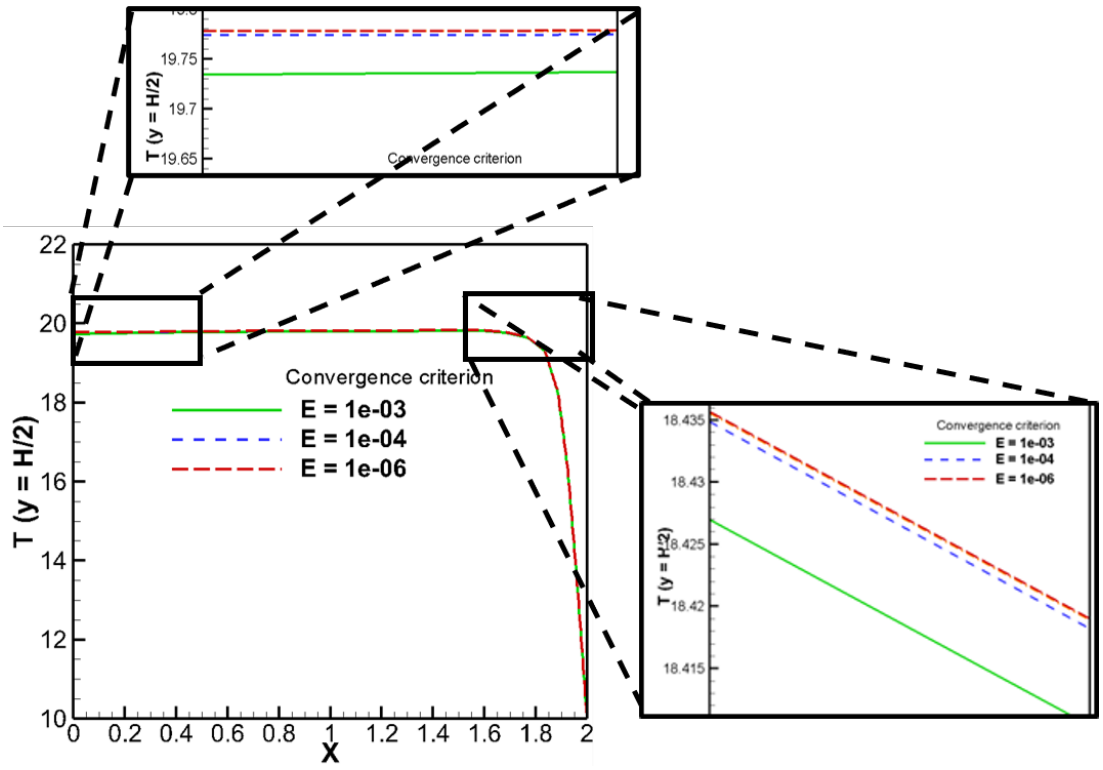

Figure 4: Comparison of axial variation of the temperature at $y = H/2$ for using different convergence criterion ($10^{-3}, 10^{-4}$ and 10^{-6}) with zoomed section from $x = 0$ to $x = 0.04$ and $x = 1.8788$ to $x = 1.8795$

2.3 Heat flux and temperature distribution

In Figure 5(a) and (b), the conductive and convective heat flux along with temperature distribution is plotted on the computational domain, respectively. The velocity ($U_A = 1$) and temperature ($T_A = 20°C$) applied at inlet starts penetrating the whole domain. As observed from Fig. 5(a), the convective heat flux vectors (($\dot{a_x} = \rho UT$) and ($\dot{a_y} = \rho VT$)) are pointing towards the postive x - direction from inlet. As the temperature difference exists between the inlet and right side boundary, the diffusion phenomena starts occuring, when the heat flow reaches the nearer the right boundary. This can be seen from the density of the conductive heat flux ($\dot{q_x} = -k(\partial T/\partial x)$ and $\dot{q_y} = -k(\partial T/\partial y)$) vectors nearer the right boundary, as shown in Fig. 5(b). The insulation boundary conditions applied on top, bottom and left wall (remaining part from the inlet section) are satisfied from the temperature distribution. The reason behind the almost uniform higher temperature throughout the domain is mainly due to lower value of diffusion coefficient or higher domaince of convective pheonomena compare to diffusion.

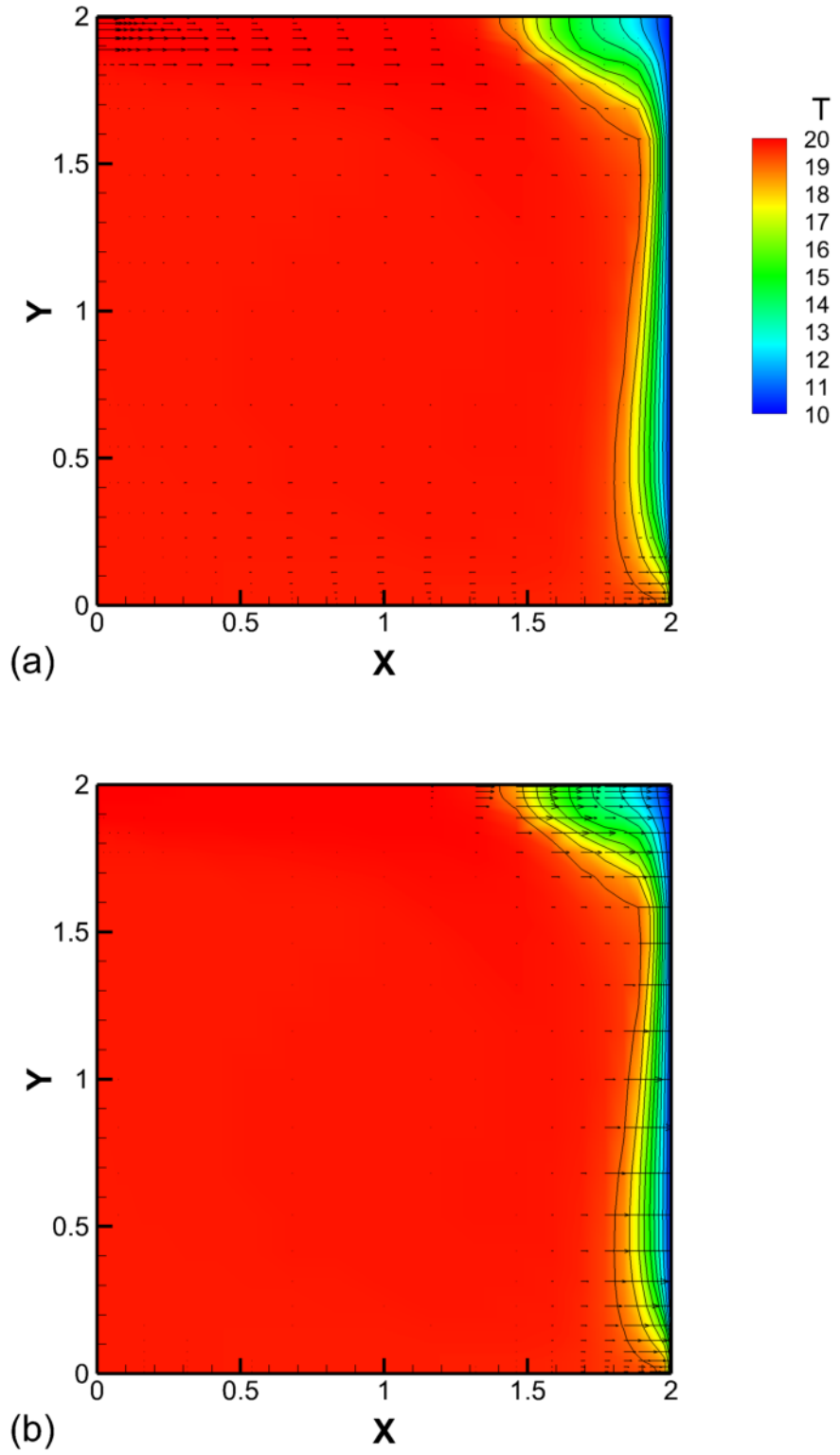

Figure 5: Temperature contour along with convective flux vectors in (a) and with conductive flux vectors in (b)

2.4 Effect of change in neumann to dirichlet boundary condition for bottom wall (answer of first question)

As discussed the boundary conditions for the second problem (Fig. 1(b)) in Subsec. 1.2, we considered bottom wall temperature (dirichlet boundary condition ($T_{bottom} = 15$)) equal to 15. We analysed the temperature distribution and heat flux for the change in one of boundary condition. It can be seen in Fig. 6 that the temperature distribution nearer inlet and right side of the geometry remains same that of previous one (Fig. 5(a)). The nature of the convective heat flux vectors are also almost same, pointing towards the postive x - direction from inlet, as observed from Fig. 6(a). On the bottom wall, the application of constant temperature ($T_{bottom} = 15$) instead of insulation, induced the diffusion or low temperature gradient (nearer the bottom wall) from bottom wall to upwards into the domain. The almost uniform temperature observed throughout the left half part of the domain in previous case ((Fig. 5(a))), is now changed due to additional diffusion occurs from the bottom wall. This observation is clearly reflected in form of conductive heat flux vector in the Fig. 6(b). The low temperature gradient can be reason behind the low value of conduction heat flux at bottom wall.

2.5 Effect of change in neumann to dirichlet boundary condition for top wall (answer of first question)

As discussed the boundary conditions for the third problem (Fig. 1(c)) in Subsec. 1.2, we considered top wall temperature (dirichlet boundary condition ($T_{top} = 15$)) equal to 15. We analysed the temperature distribution and heat flux for the change in one of boundary condition. It can be seen in Fig. 7 that the temperature distribution close to inlet and right side of the geometry remains same that of previous one (Fig. 5(a)). The nature of the convective heat flux vectors are also almost same, pointing towards the postive x - direction from inlet, as observed from Fig. 7(a). On the top wall, the application of constant temperature ($T_{top} = 15$) instead of insulation, induced the diffusion or low temperature gradient (nearer the bottom wall) from top wall to downwards into the domain. The almost uniform temperature observed throughout the left half part of the domain in previous case ((Fig. 5(a))), is now changed due to additional diffusion occurs from the top wall. This observation is clearly reflected in form of conductive heat flux vector in the of Fig. 7(b). The low temperature gradient can be reason behind the low value of conduction heat flux at top wall. The influence of dirichlet boundary condition on top wall is highly effective to reduce the inlet velocity driven dominance in the domain compare to dirichelet boundary condition on bottom wall (Fig. 6(b)).

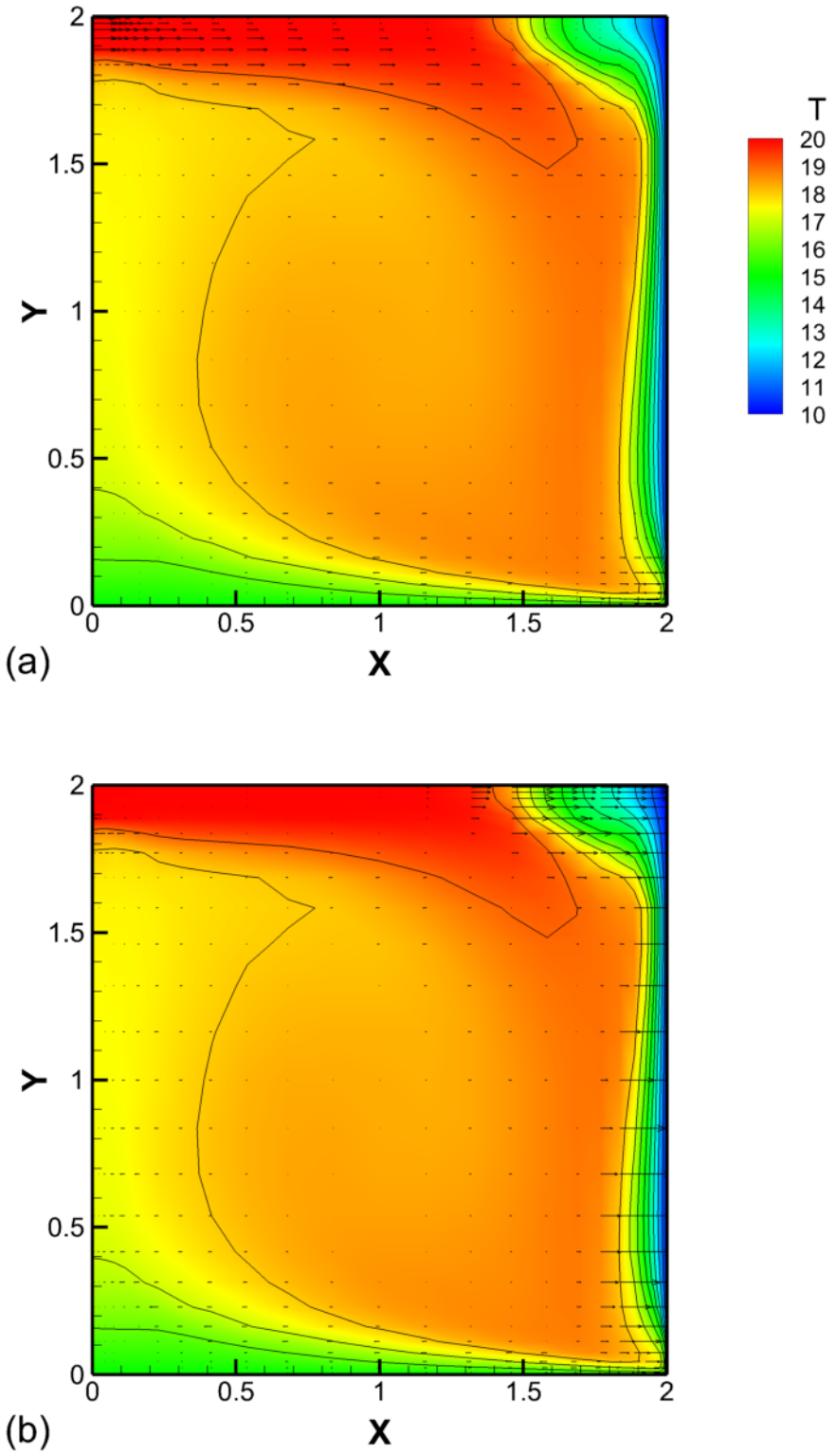

Figure 6: Temperature contour along with convective flux vectors in (a) and with conductive flux vectors in (b), for change in neuman to dirichlet boundary condition on bottom wall

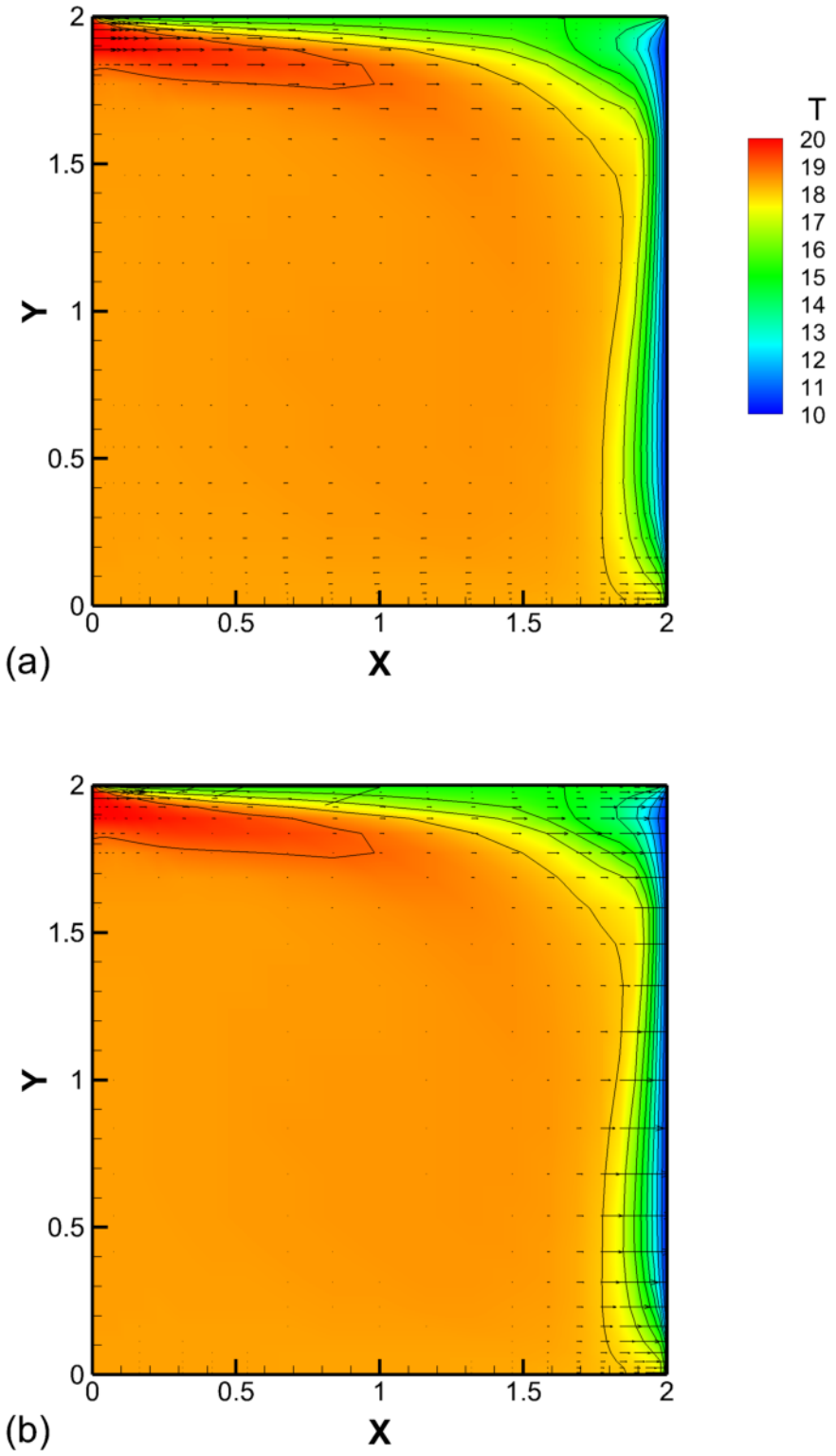

Figure 7: Temperature contour along with convective flux vectors in (a) and with conductive flux vectors in (b), for change in neuman to dirichlet boundary condition on top wall

2.6 Total heat flux through all the boundaries

As per boundary condition given for the first problem (Fig. 1(a)) in Subsec. 1.2, we calculated the convective and conductive heat flux on inlet, outlet and wall - boundaries. The total x-direction (from the left and right boundary) and y-direction (top and bottom boundary) convective heat flux are calculated using following equation 2. The same way total x-direction (from the left and right boundary) and y-direction (top and bottom boundary) conductive heat flux are calculated using equation 3.

$$\Big[(\rho UT)_{left\ bc} - (\rho UT)_{right\ bc}\Big] + \Big[(\rho VT)_{top\ bc} - (\rho VT)_{bottom\ bc}\Big] \tag{2}$$

$$\left[\left(-\Gamma\frac{\partial T}{\partial x}\right)_{left\ bc} - \left(-\Gamma\frac{\partial T}{\partial x}\right)_{right\ bc}\right] + \left[\left(-\Gamma\frac{\partial T}{\partial y}\right)_{top\ bc} - \left(-\Gamma\frac{\partial T}{\partial y}\right)_{bottom\ bc}\right] \tag{3}$$

The value of total convective flux is 50 W/m^2 and total conductive heat flux is -12.046 W/m^2. So, total heat flux through all the boundary is 37.79 W/m^2.